2D Materials

PAPER

A monolayer MoS_2 p-n homogenous photodiode with enhanced photoresponse by piezo-phototronic effect

To cite this article: Ke Zhang *et al* 2018 *2D Mater.* **5** 035038

2D Materials

CrossMark

RECEIVED
13 April 2018

REVISED
26 May 2018

ACCEPTED FOR PUBLICATION
1 June 2018

PUBLISHED
13 June 2018

PAPER

A monolayer MoS_2 p-n homogenous photodiode with enhanced photoresponse by piezo-phototronic effect

Ke Zhang[1,2,3], Junyi Zhai[1,3,5] and Zhong Lin Wang[1,3,4]

[1] CAS Center for Excellence in Nanoscience, Beijing Key Laboratory of Micro-nano Energy and Sensor, Beijing Institute of Nanoenergy and Nanosystems, Chinese Academy of Sciences, Beijing 100083, People's Republic of China
[2] CAS Center for Excellence in Nanoscience, National Center for Nanoscience and Technology, Beijing 100190, People's Republic of China
[3] School of Nanoscience and Technology, University of Chinese Academy of Sciences, Beijing 100049, People's Republic of China
[4] School of Materials Science and Engineering, Georgia Institute of Technology, Atlanta, GA 30332, United States of America
[5] Center on Nanoenergy Research, School of Physical Science and Technology, Guangxi University, Nanning 530004, People's Republic of China

E-mail: jyzhai@binn.cas.cn and zhong.wang@mse.gatech.edu

Keywords: TMDCs, piezoelectricity, p-n homojunction, piezo-phototronic effect, enhanced photoresponse

Supplementary material for this article is available online

Abstract

Transition-metal dichalcogenides (TMDCs) have recently open a new perspective in electronics and optoelectronics due to their unique planar crystal structures and incredible physical characteristics. Strong in-plane piezoelectricity is their unique property owing to non-centrosymmetric structure, differing from other two dimension (2D) materials, such as graphene and black phosphorus. In this work, we develop a flexible photodiode based on monolayer MoS_2 lateral p-n homojunction with significant enhancement in photoresponsivity and detectivity. Piezo-phototronic effect is used to achieve this enhancement by adjusting the barrier height and broadening depletion zone at p-n junction interface under external strain. The wider depletion zone benefits the separation and transport of photogenerated carriers, thus enhancing the photocurrent. When a 0.51% external static tensile strain was applied, the photoresponsivity and detectivity are improved up to 1162 A W^{-1} and 1.72×10^{12} Jones, with about 619% and 319% enhancement compared with strain-free state, respectively. Consequently, this work provides an effective strategy to utilize unavoidable external strain to improve TMDCs-based optoelectronic devices performance. At the same time, it has reference meaning to achieve flexible, low-consumption and high-performance 2D devices without electric gate-control.

1. Introduction

Flexible, ultrathin and transparent will be key characteristics of the next-generation semiconductor electronics and optoelectronics. Two-dimensional (2D) materials are promising candidates for new wearable devices, flexible sensing and health monitoring [1–7]. Molybdenum disulfide (MoS_2), typical representative of 2D TMDCs, is one of the best choices of the host materials in optoelectronics because of its good stability, high mechanical strength and adjustable band gap. Monolayer MoS_2 has superior semiconductor properties and a 1.8 eV direct band-gap, leading to excellent switching and photoresponse characteristics [8–15]. However, the limited excitation efficiency and non-negligible photogenerated carriers' recombination are the obstacles to the photoelectric performance of the MoS_2-based devices. Electric gate-control is an usual and efficient approach to control carriers transportation and improve devices performance [16–19]. Without the assistance of gate voltage, the device will have only poor performance or be worthless. However, electric gate regulation requires not only high power consumption but also extreme operating conditions. At present, available gate regulation usually exists in devices on hard substrates because there are still no high-quality flexible gate dielectric materials. It is desired to achieve operative regulation and high devices performance in flexible conditions.

Recently, piezoelectricity in odd layer MoS_2 owing to its non-centrosymmetric structure was observed

in experiments [8, 20]. Based on the strong in-plane piezoelectricity in MoS_2, piezo-phototronic effect is regarded as a novel and efficient regulation method for carriers' generation, transport, separation, and/or recombination, especially in flexible optoelectronics [8, 21, 22]. In details, piezo-phototronic effect is that, under external strain stimulation, piezoelectric polarization charges accumulated at the p-n junction interface or metal–semiconductor interface and produce piezoelectric potential, which adjusts band structure at interface and modulates photogenerated carriers' generation, transport, separation, and/or recombination. Compared to transitional electric gate-control (external gate), piezo-phototronic effect can be considered as 'internal gate', which is more substantive and low power consumption. Meanwhile, the inevitable strain from flexible substrate can be used to enhance the performance of optoelectronic devices. In order to achieve better behaviours of MoS_2-based flexible optoelectronic devices via piezo-phototronic effect, an ideal interface barrier is crucial to obtain better piezo-phototronic performance. Constructing p-n homojunction in MoS_2 is a worthwhile strategy because of it provides a high-efficiency interface barrier for piezoelectric modulation and benefits photogenerated carriers' separation. In addition, a homojunction has sharper interface and lower resistance conductive path than heterojunction [23–26].

In this work, we successfully fabricated a flexible monolayer MoS_2 lateral p-n diode and enhanced the device photoresponse performance by applying external strain based on piezo-phototronic effect. The selective part of the triangle monolayer MoS_2 is changed for p-type conduction by chemical doping and forms a p-n homojunction with remnant initial n-type MoS_2. Under external strain, the opposite piezoelectric potential in two sides of homojunction interface will adjust the band structure and extend the depletion zone, thus enhancing the separation efficiency of photogenerated electron-hole pairs and improving the photoresponse performance. When a 0.51% static tensile strain was applied, the photoresponsivity and detectivity of our photodiode was improved up to 1162 A W^{-1} and 1.72×10^{12} Jones, respectively, with 619% and 319% enhancements compared to no strain state. This work provides a novel design concept to developing flexible 2D TMDCs-based optoelectronic devices with strain regulation. Moreover, this paper gives detailed discussion on intrinsic mechanism of piezo-phototronic effect and it is referenceable to apply the piezoelectricity of TMDCs to various optoelectronic fields, such as photodetection, environment response and strain sensing.

2. Methods

Figure 1 exhibits the fabrication processes of flexible MoS_2 lateral p-n homojunction diodes. Large-scale and triangle monolayer MoS_2 nanosheets were first synthesized on SiO_2/Si substrates via CVD methods [27]. High-quality MoS_2 flakes were confirmed by optical images and TEM as well as corresponding selected area electron diffraction (SAED) pattern (figure S1(a) and (b) (stacks.iop.org/TDM/5/035038/mmedia)). Triangle MoS_2 was the most energetically stable existent morphology, and it allowed us to easily identify the lattice orientation from optical images (figure 1(a)). The boundary of the doped region was designed to be perpendicular to the armchair direction of MoS_2 single crystal, as shown in figure 1(b). Polymethyl methacrylate (PMMA) is regarded as a shielding layer, and the doped area can be accurately etched by electron beam lithography (EBL) to obtain a better defined and more regular interface with two sides. A thin layer of the $AuCl_3$ solution was spin-coated above the PMMA shielding layer, followed by annealing at 100 °C for 30 min in Ar atmosphere (figure 1(c)). $AuCl_3$ solution was doped in the required area, and the other area was blocked by PMMA. After dissolving PMMA, the monolayer MoS_2 p-n homojunction based on the SiO_2/Si substrate was finished, and the doping details are illustrated in supporting information. To construct a flexible p-n diode, the as-fabricated MoS_2 homojunction was transferred to a flexible polyethylene terephthalate (PET) substrate by the mature wet-transfer method, as reported previously (figures 1(d)–(e)). Finally, Cr/Au electrodes (5 nm/50 nm) were patterned and deposited on two sides of the p-n homojunction to provide ohmic contact by EBL and electron beam evaporation deposition (figure 1(f)).

3. Results and discussions

A monolayer MoS_2 lateral homogeneous p-n diode is first constructed on a SiO_2/Si substrate. Figure 2(a) depicts the schematic diagram of p-n diode and chemical doping mechanism. $AuCl_3$ solution is regarded as a stable dopant providing a p-type doping effect because it has a larger reduction potential with a greater tendency to accept electrons [28, 29]. Au^{3+} can be reduced to Au particles by surface charge transfer from MoS_2, which results in the p-type doping behaviour of monolayer MoS_2, according to the following reaction.

$$AuCl_4^- + 3e^- \rightarrow Au + 4Cl^-. \quad (1)$$

This surface doping will raise the work function of the doping region and lead to a significant potential difference at the interface between doped MoS_2 and pristine MoS_2 (without doping). The electrons of the pristine area tend to flow to the p-type doped area and holes, conversely, forming an effective p-n junction. In terms of morphology, figure 2(b) shows the optical image of monolayer MoS_2 lateral p-n homojunction. Obviously, the doped area has a deeper colour contrast compared to pristine MoS_2, forming a sharp and distinct interface. We also investigated the microscopic morphologies of the doping region by transmission electron microscope (TEM)

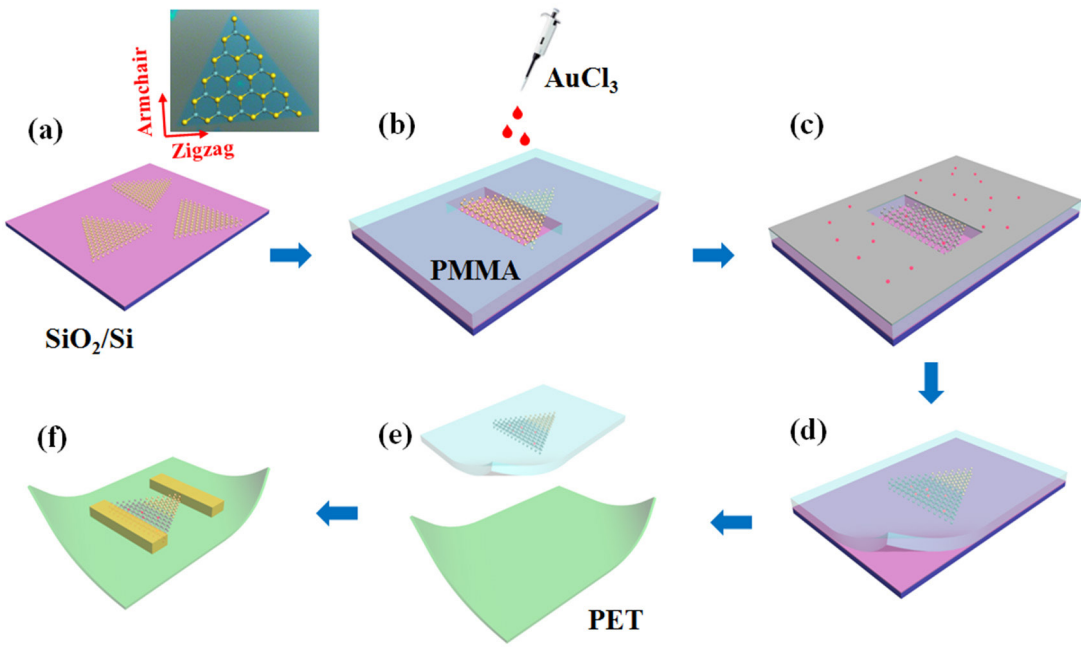

Figure 1. The processes of flexible MoS_2 p-n homogenous photodiode. (a) CVD-grown monolayer triangle MoS_2 on a SiO_2/Si substrate. The optical image shows the lattice orientation. (b) Spin-coated $AuCl_3$ solution on the PMMA shielding layer after etching. (c) Annealing for 30 min in Ar atmosphere. (d) Stripping the MoS_2 p-n homojunction from the SiO_2/Si substrate with the assistance of PMMA. (e) Transferring MoS_2 to a flexible PET substrate. (f) Patterning and depositing Cr/Au electrodes.

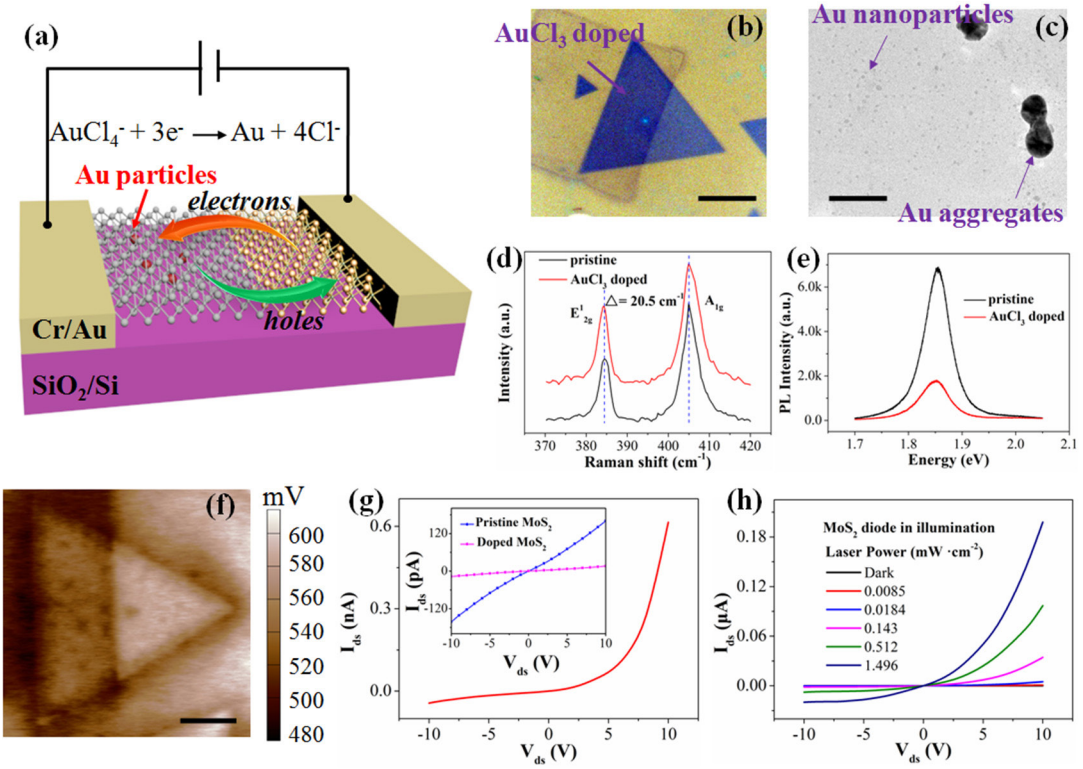

Figure 2. Basic doping mechanism and device performance. (a) The schematic diagram of monolayer MoS_2 p-n homogenous diode. (b) The optical image of CVD-grown monolayer MoS_2 after partial $AuCl_3$ doping. The scale bar is 20 μm. (c)TEM morphology of chemically doped MoS_2. The scale bar is 100 nm. (d) and (e) Raman and PL spectra comparisons between pristine $MoS_2$and doped MoS_2 under 532 nm laser excitation. (f) Surface electric potential of the monolayer MoS_2 homojunction. The scale bar is 20 μm. (g) Rectification characteristic of the MoS_2 p-n homojunction. The inset shows the *I*–*V* characteristics of pristine and doped MoS_2. (h) Photoresponse performance of the diode in dark and various illumination intensities.

(figure 2(c)), indicating that Au nanoparticles or aggregates generated by the reduction of $AuCl_4^-$ uniformly distribute and attach on the surface of MoS_2. Regarding the optical characteristics, the Raman peaks of the doped area have almost the same positions (in-plane mode E^1_{2g} (384.4 cm^{-1}) and out-of-plane mode A_{1g} (404.9 cm^{-1}), $\Delta = 20.5\,cm^{-1}$) with pristine MoS_2, indicating that there is no obvious influence on phonon-electron coupling after surface doping (figure 2(d)) [30]. The typical photoluminescence (PL) spectrum of the pristine CVD-grown monolayer MoS_2 in figure 2(e) has a high intensity peak at 670 nm (1.85 eV), corresponding to a direct gap optical transition [31]. In contrast, the PL intensity of the $AuCl_3$ doped region is significantly weakened due to low electron concentration after doping. To clearly reveal the p-type doping effect, the photoelectric properties of p-n homojunction are tested, including the surface electric potential, current–voltage (I–V) curves and photoresponse behaviour. The surface electric potential is characterized by scanning Kelvin probe microscopy (SKPM), as shown in figure 2(f). The doped area has nearly a 60 mV surface electric potential difference with the pristine region. The lower the surface potential is, the higher the work function is, creating an available barrier between the p-type doped region and the pristine region. More intuitively, the monolayer MoS_2 diode displays a favourable p-n junction rectification characteristic (figure 2(g)). Moreover, the I–V curves of the individual pristine and doped regions were also tested (figure 2(g), inset). Both exhibit ohmic contact characteristics, demonstrating that there is no obvious electrical barrier between MoS_2 and the electrodes, regardless of the region type. The photoresponse measurement of the monolayer MoS_2 p-n diode on a SiO_2/Si substrate was performed under variable optical power intensity (figure 2(h)). The output light current (I_{light}) of the as-fabricated diode increased from 0.6 nA (dark, $V_{ds} = 10$ V) to 0.2 μA (1.496 mW cm^{-2}, $V_{ds} = 10$ V) and had a high on–off ratio, showing that it is adaptable for photodetector and other optoelectronic devices. Compared with the pure monolayer MoS_2 photodetector, the p-n homojunction photodiode certainly has more efficient photogenerated carriers' separation, leading to better device performance (figures S2(a) and (b)).

Based on as-fabricated flexible monolayer MoS_2 homogenous p-n photodiode, the photoresponse performances were measured under variable optical power intensities and different external strains, with the results summarized in figure 3. All the electrical characteristics measurements were operated on a home-made high-precision manual translation table under 532 nm laser illuminations (figure 3(a)). The external strain was loaded via bending the PET substrate by moving the transition tables precisely towards each other, and the MoS_2 p-n photodiode can be located accurately with the assistance of a charge-coupled device (CCD) imaging system to ensure the proper force direction. The photoresponse of the monolayer MoS_2 p-n photodiode was first performed in dark and various illumination intensities without loading strain (figure 3(b)). The light current (I_{light}) increased step-by-step with increasing luminous intensity and maintained stable p-n junction rectification characteristics. At a bias of −10 V, the photodiode had an ultra-low dark current (I_{dark}) of nearly 70 pA. Such small dark current is mainly attributed to the depletion of electrons after p-type doping and high-surface roughness of the PET substrate. The output current is improved to 190 nA when the device is illuminated with a laser intensity of 7.41 mW cm^{-2}, and the on/off ratio can reach approximately 3×10^3, indicating that the p-n photodiode retained the high photoresponse behaviours after being transferred to the flexible polymer substrate. The photoresponse performance of flexible MoS_2 photodiode was also tested with the application of different static tensile strains. Under strain conditions, the current was enhanced due to the piezo-phototronic effect, which adjusts the band structure at the p-n homojunction interface and further improves the separation efficiency of the photogenerated electron-hole pairs. Figure 3(c) shows the change in the light current of the photodiode at the same optical power intensity (0.0085 mW cm^{-2}) with increasing tensile strains. The output current exhibits a substantial increase as the external tensile strain increased from 0% to 0.51%, and the current output under 0.51% tensile strain showed approximately a 5-fold improvement compared to the strain-free state. In addition, the photocurrent values ($I_{ph} = I_{light} - I_{dark}$) at −10 V bias under different tensile strains and various illumination intensities are summarized and presented in figure 3(d), and it is shown that the external static strain can effectively improve the photoresponse performance of flexible MoS_2 homogenous photodiodes under the same illumination conditions. Photoresponsivity (R) is a critical photodetector parameter that is calculated by equation (2), where P is the optical power density, and A is the available illuminated area on the photodiode.

$$R = \frac{I_{ph}}{P_i \cdot A} = \frac{I_{light} - I_{dark}}{P_i \cdot A} \tag{2}$$

$$D^* = \frac{R}{\sqrt{\frac{2qI_{dark}}{A}}} = \frac{I_{ph}}{P_i \cdot \sqrt{2AqI_{dark}}}. \tag{3}$$

The photoresponsivity decreases with increasing illumination intensity due to trap states present inside the MoS_2 or at the interface of MoS_2 and the substrate [11, 22]. Moreover, the photoresponsivity of the photodiode reached a maximum value in lowest optical power intensity (0.0085 mW cm^{-2}), and it was enhanced from 189 A W^{-1} under no strain state up to 1162 A W^{-1} under a 0.51% tensile strain by the piezo-phototronic effect (figure 3(e)).It should be noted that external strain has a more significant effect on photoresponsivity at a relatively low illumination

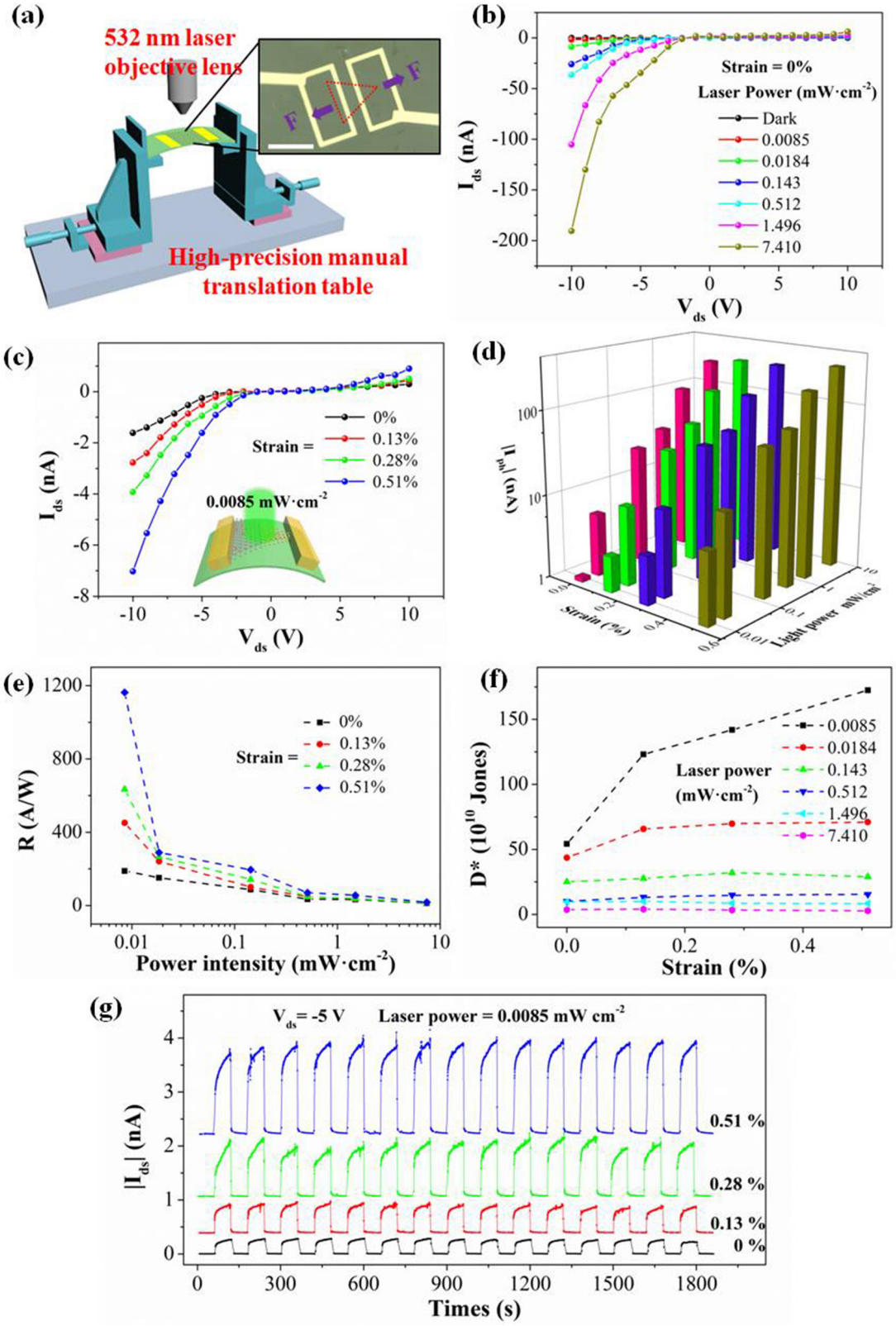

Figure 3. Photoresponse behaviours enhanced by piezo-phototronic effect. (a) Home-made high-precision table for loading strain. The optical image presents a practical device structure (MoS_2 is outlined by red dash line). (b) Photoresponse performance under the strain-free state. (c) *I–V* characteristics under the same illumination intensity (0.0085 mW cm^{-2}) under different static tensile strains. (d)–(f) The variations in value of the photocurrent (I_{ph}), photoresponsivity (R) and detectivity (D^*) at a bias of -10 V under different strains and various optical power intensities. (g) Time-dependent photoresponse of the photodiode to periodic on/off illuminations under different tensile strains.

intensity, which is attributed to the screening effect of the amount of free charges under high-intensity illumination offsetting the piezoelectric polarization charges. Another evaluation criterion is detectivity (D^*), which is defined as equation (3), where q is the electronic charge. In figure 3(f), the D^* increases with external strain under a weak illumination of 0.0085 mW cm^{-2} and reaches a maximum value of 1.72×10^{12}

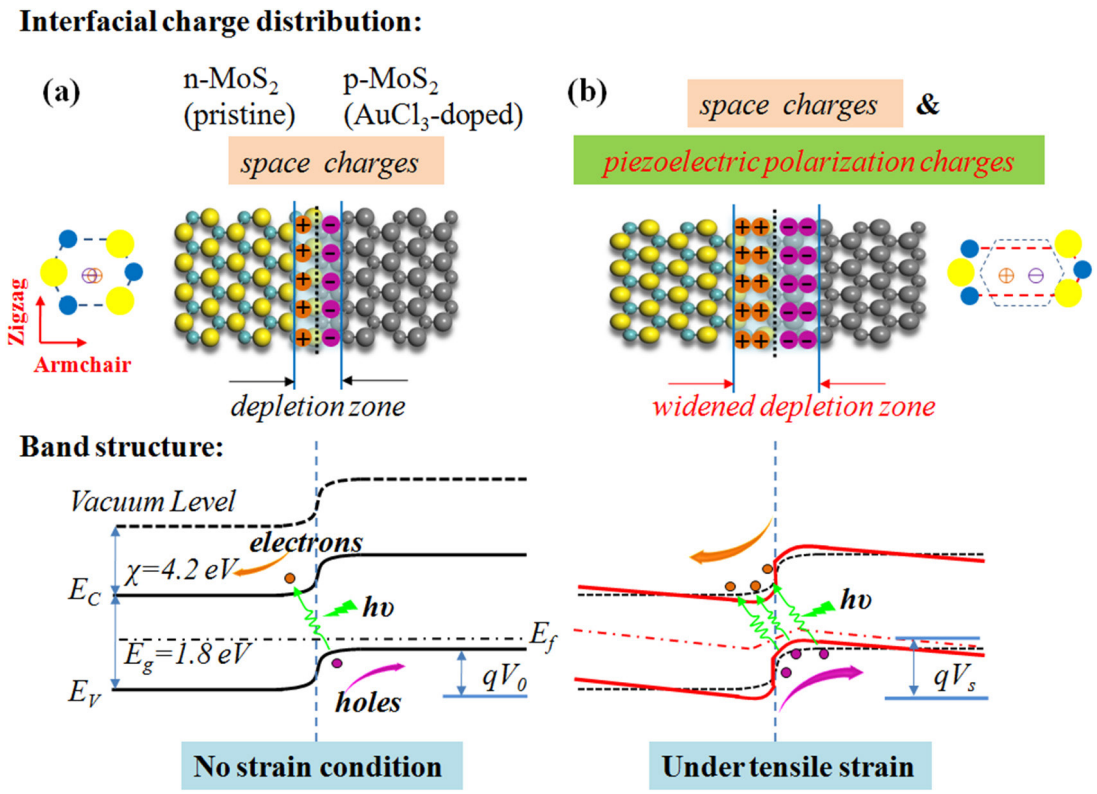

Figure 4. Work mechanisms of strain modulating MoS_2 p-n homojunction. Piezoelectric polarization charge distribution and band structure at the interface of the MoS_2 p-n photodiode under (a) no strain state and (b) static tensile strain state.

Jones. There is an available enhancement in strain-free state (5.4×10^{11} Jones). The time dependence of the photoresponse of the photodiode under periodic on/off illumination was also studied under external strain. Figure 3(g) presents the periodic photoresponse ($V_{ds} = -5$ V) under different tensile strains and 0.0085 mW cm^{-2} 532 nm laser illumination and the device performs an excellent operational stability for photodetection.

To elucidate the piezo-phototronic effect on enhancing the device photoresponse performances, the physical mechanisms were presented and discussed in detail (figure 4). The charge distributions and energy band diagrams at the interface of the monolayer p-n homojunction with the source-drain bias under the strain-free state and static tensile strain state are presented in figures 4(a) and (b), respectively. Pristine monolayer MoS_2 has 4.2 eV electron affinity and 1.8 eV band-gap [32]. The original CVD-grown MoS_2 performs with weak n-type characteristics, and its Fermi level is usually located between the conduction band and valence band. After p-type doping, the electron concentration of the doped area decreases, and the work function increases, causing a downward shift of the Fermi level approaching the valence band, as shown in the band diagram of figure 4(a). Without loading strain, there are no piezoelectric polarization charges distributed at the p-n junction interface because the positive charge centre and negative charge centre coincide. The unique available charges around the junction region are space charges, which come from ionized donors or ionized acceptors (figure 4(a), charge distribution). The positive and negative space charges form a built-in electric potential (V_0) at the p-n interface, effectively separating photogenerated electron-hole pairs under illumination (figure 4(a), band structure). When an external strain is loaded on the device, the monolayer MoS_2 is stretched, leading to the detachment of the positive and negative charges centres because of its non-centrosymmetric structure. The piezoelectric potential induced by the polarization charges at the p-n homojunction interface will modulate the band structure and affect carriers generation, transport, separation or recombination. In detail, as shown in figure 4(b) (band structure), the positive piezoelectric potential induced by the polarization charges on the pristine MoS_2 area side lowers the bands near the interface (left side), and the negative piezoelectric potential created on the doped MoS_2 area side raises the bands near the interface (right side), increasing the barrier height (qV_s) and widening the depletion zone. This provides an extra driving force to separate the photogenerated electrons and holes, and it reduces recombination as well as accelerates carrier transportation, thus enhancing the photocurrent and improving the photoresponse performance of the device.

Table S1 summarizes and compares the photoresponse performance of previously reported rigid or flexible MoS_2-based photodetectors with that of the p-n homogenous photodiodes in this work [10, 21, 33–38]. For the devices on rigid substrates, electric gate regulation is regarded as a necessary

means to obtain high performance, whether it is a continuous top gate and back gate voltage, or a voltage pulse. In addition, it is difficult to achieve a good and steady photoresponse performance for the flexible devices because of the lack of external gate regulation and other specific obstacles existing in the flexible applications. Comparatively, with the combined effects of the p-n homojunction and piezo-phototronic characteristics, the flexible p-n homogenous photodiode in this work has appreciable and balanced photoresponse performance in multiple parameters, making the best use of the special characteristics in 2D materials.

4. Conclusion

In summary, we first designed and fabricated a flexible lateral p-n homogenous photodiode based on a monolayer MoS_2. This device provided significant enhancement in the photoresponse performance under external strain utilizing the piezo-phototronic effect, which modulates the band structure at the interface and helps the separation and transport of photogenerated carriers. The photoresponsivity was improved by 619%, from 189 A W^{-1} to 1162 A W^{-1} with the loading of a 0.51% tensile strain. Meanwhile, the detectivity was also enhanced by 319% and reached up to 1.72×10^{12} Jones in low-intensity illumination. This work provides a new route to use the particular piezoelectricity of 2D TMDCs (such as MoS_2, $MoSe_2$, $MoTe_2$, etc) to enhance device performance. By coupling mechanics, photics and electricity, it is anticipated and more competitive for nanoelectronics in fields of flexible sensing and ultra-thin optoelectronics.

Acknowledgments

This work was supported by National Key R & D Project from Minister of Science and Technology, China (2016YFA0202703, 2016YFA0202704); NSFC 51472056; the 'thousands talents' Program for Pioneer Researcher and Their Innovation Team, China; and the Recruitment Program of Global Youth Experts, China.

ORCID iDs

Junyi Zhai https://orcid.org/0000-0001-8900-4638
Zhong Lin Wang https://orcid.org/0000-0002-5530-0380

References

[1] Xia F, Wang H, Xiao D, Dubey M and Ramasubramaniam A 2014 Two-dimensional material nanophotonics *Nat. Photon.* **8** 899
[2] Akinwande D, Petrone N and Hone J 2014 Two-dimensional flexible nanoelectronics *Nat. Commun.* **5** 5678
[3] Wang Q H, Kalantar-Zadeh K, Kis A, Coleman J N and Strano M S 2012 Electronics and optoelectronics of two-dimensional transition metal dichalcogenides *Nat. Nanotechnol.* **7** 699
[4] Zhang W, Wang Q, Chen Y, Wang Z and Wee A T S 2016 Van der Waals stacked 2D layered materials for optoelectronics *2D Mater.* **3** 022001
[5] Sang J K, Choi K, Lee B, Kim Y and Hong B H 2015 Materials for flexible, stretchable electronics: graphene and 2D materials *Annu. Rev.Mater. Res.* **45** 63
[6] Novoselov K S, Mishchenko A, Carvalho A and Castro Neto A H 2016 2D materials and van der Waals heterostructures *Science* **353** 461
[7] Sommer Thygesen K 2017 Calculating excitons, plasmons, and quasiparticles in 2D materials and van der Waals heterostructures *2D Mater.* **4** 022004
[8] Wu W *et al* 2014 Piezoelectricity of single-atomic-layer MoS2 for energy conversion and piezotronics *Nature* **514** 470
[9] Peng B, Yu G, Liu X, Liu B, Liang X, Bi L, Deng L, Sum T C and Loh K P 2016 Ultrafast charge transfer in MoS_2/WSe_2 p–n Heterojunction *2D Mater.* **3** 025020
[10] Lopez-Sanchez O, Lembke D, Kayci M, Radenovic A and Kis A 2013 Ultrasensitive photodetectors based on monolayer MoS_2 *Nat. Nanotechnol.* **8** 497
[11] Radisavljevic B, Radenovic A, Brivio J, Giacometti V and Kis A 2011 Single-layer MoS_2 transistors *Nat. Nanotechnol.* **6** 147
[12] Perealópez N, Lin Z, Pradhan N R, Iñiguezrábago A, Elías A L, Mccreary A, Lou J, Ajayan P M, Terrones H and Balicas L 2014 CVD-grown monolayered MoS_2 as an effective photosensor operating at low-voltage *2D Mater.* **1** 011004
[13] Bertolazzi S, Brivio J and Kis A 2011 Stretching and breaking of ultrathin MoS_2 *ACS Nano* **5** 9703
[14] Mak K F, Lee C, Hone J, Shan J and Heinz T F 2010 Atomically thin MoS_2: a new direct-gap semiconductor *Phys. Rev. Lett.* **105** 136805
[15] Illarionov Y Y, Rzepa G, Waltl M, Knobloch T, Grill A, Furchi M M, Mueller T and Grasser T 2016 The role of charge trapping in MoS_2/SiO_2 and MoS_2/h-BN field-effect transistors *Z. Phys.* C **3** 035004
[16] Kufer D, Nikitskiy I, Lasanta T, Navickaite G, Koppens F H L and Konstantatos G 2015 Hybrid 2D–0D MoS_2–PbS quantum dot photodetectors *Adv. Mater.* **27** 176
[17] Cheng R, Li D, Zhou H, Wang C, Yin A, Jiang S, Liu Y, Chen Y, Huang Y and Duan X 2014 Electroluminescence and photocurrent generation from atomically sharp WSe_2/MoS_2 heterojunction p-n diodes *Nano Lett.* **14** 5590
[18] Roy K, Padmanabhan M, Goswami S, Sai T P, Ramalingam G, Raghavan S and Ghosh A 2013 Graphene-MoS_2 hybrid structures for multifunctional photoresponsive memory devices *Nat. Nanotechnol.* **8** 826
[19] Zhang W, Chuu C P, Huang J K, Chen C H, Tsai M L, Chang Y H, Liang C T, Chen Y Z, Chueh Y L and He J H 2014 Ultrahigh-gain photodetectors based on atomically thin graphene-MoS_2 heterostructures *Sci. Rep.* **4** 3826
[20] Zhu H, Wang Y, Xiao J, Liu M, Xiong S, Wong Z J, Ye Z, Ye Y, Yin X and Zhang X 2015 Observation of piezoelectricity in free-standing monolayer MoS_2 *Nat. Nanotechnol.* **10** 151
[21] Zhang K 2017 A flexible p-CuO/n-MoS_2 heterojunction photodetector with enhanced photoresponse by the piezo-phototronic effect *Mater. Horiz.* **4** 274
[22] Wu W, Wang L, Yu R, Liu Y, Wei S-H, Hone J and Wang Z L 2016 Piezophototronic effect in single-atomic-layer MoS_2 for strain-gated flexible optoelectronics *Adv. Mater.* **28** 8463
[23] Zhao Y, Xu K, Pan F, Zhou C, Zhou F and Chai Y 2017 Doping, contact and interface engineering of two-dimensional layered transition metal dichalcogenides transistors *Adv. Funct. Mater.* **27** 1604638
[24] Zhang X, Shao Z, Zhang X, He Y and Jie J 2016 Surface charge transfer doping of low-dimensional nanostructures toward high-performance nanodevices *Adv. Mater.* **28** 10409
[25] Li H-M, Lee D, Qu D, Liu X, Ryu J, Seabaugh A and Yoo W J 2015 Ultimate thin vertical p–n junction composed of two-dimensional layered molybdenum disulfide *Nat. Commun.* **6** 6564
[26] Choi M S, Qu D, Lee D, Liu X, Watanabe K, Taniguchi T and Yoo W J 2014 Lateral MoS_2 p-n junction formed by chemical doping for use in high-performance optoelectronics *ACS Nano* **8** 9332

[27] van der Zande A M, Huang P Y, Chenet D A, Berkelbach T C, You Y, Lee G-H, Heinz T F, Reichman D R, Muller D A and Hone J C 2013 Grains and grain boundaries in highly crystalline monolayer molybdenum disulphide *Nat. Mater.* **12** 554
[28] Shin H J, Choi W M, Choi D, Gang H H, Yoon S M, Park H K, Kim S W, Yong W J, Sang Y L and Kim J M 2010 Control of electronic structure of graphene by various dopants and their effects on a nanogenerator *J. Am. Chem. Soc.* **132** 15603–9
[29] Shi Y, Kim K K, Reina A, Hofmann M, Li L J and Kong J 2010 Work function engineering of graphene electrode via chemical doping *ACS Nano* **4** 2689
[30] Li H, Zhang Q, Yap C C R, Tay B K, Edwin T H T, Olivier A and Baillargeat D 2012 From bulk to monolayer MoS_2: evolution of raman scattering *Adv. Funct. Mater.* **22** 1385
[31] Splendiani A, Sun L, Zhang Y, Li T, Kim J, Chim C-Y, Galli G and Wang F 2010 Emerging photoluminescence in monolayer MoS_2 *Nano Lett.* **10** 1271
[32] Bertolazzi S, Krasnozhon D and Kis A 2013 Nonvolatile memory cells based on MoS_2/graphene heterostructures *ACS Nano* **7** 3246
[33] De F D, Goykhman I, Yoon D, Bruna M, Eiden A, Milana S, Sassi U, Barbone M, Dumcenco D and Marinov K 2016 High responsivity, large-area graphene/MoS_2 flexible photodetectors *ACS Nano* **10** 8252
[34] Wang X *et al* 2015 Ultrasensitive and broadband MoS_2 photodetector driven by ferroelectrics *Adv. Mater.* **27** 6575
[35] Xu H, Wu J, Feng Q, Mao N, Wang C and Zhang J 2014 High responsivity and gate tunable graphene-MoS_2 hybrid phototransistor *Small* **10** 2300
[36] Kwon J, Hong Y K, Han G, Omkaram I, Choi W, Kim S and Yoon Y 2015 Giant photoamplification in indirect-bandgap multilayer MoS_2 phototransistors with local bottom-gate structures *Adv. Mater.* **27** 2224
[37] Huo N, Kang J, Wei Z, Li S S, Li J and Wei S H 2015 Novel and enhanced optoelectronic performances of multilayer MoS_2–WS_2 heterostructure transistors *Adv. Funct. Mater.* **24** 7025
[38] Pak J, Jang J, Cho K, Kim T Y, Kim J K, Song Y, Hong W K, Min M, Lee H and Lee T 2015 Enhancement of photodetection characteristics of MoS_2 field effect transistors using surface treatment with copper phthalocyanine *Nanoscale* **7** 18780